ELSEVIER

Journal of Biomechanics 40 (2007) 2788–2795

JOURNAL OF BIOMECHANICS

www.elsevier.com/locate/jbiomech
www.JBiomech.com

Micromechanics fracture in osteonal cortical bone: A study of the interactions between microcrack propagation, microstructure and the material properties

A. Raeisi Najafi[a], A.R. Arshi[a], M.R. Eslami[b], S. Fariborz[b], M.H. Moeinzadeh[c,*]

[a]*Biomedical Engineering Department, Amirkabir University of Technology, Tehran, Iran*
[b]*Mechanical Engineering Department, Amirkabir University of Technology, Tehran, Iran*
[c]*Department of Industrial and Enterprise Systems Engineering, University of Illinois at Urbana-Champaign, USA*

Accepted 24 January 2007

Abstract

A two-dimensional micromechanical fibre reinforced composite materials model for osteonal cortical bone is presented. The interstitial bone is modelled as a matrix, the osteons are modelled as fibres, and the cement line is presented as interface tissue. The interaction between osteons and microcracks is evaluated by linear elastic fracture mechanics theory, followed by a determination of the stress intensity factor at the vicinity of the microcrack tips. The results indicate that bone microstructural heterogeneity greatly influences fracture parameters. Furthermore, microstructural morphology and loading conditions affect growth trajectories, the microcrack propagation trajectory deviates from the osteon under tensile loading, and osteon penetration is observed under compressive loads.

Keywords: Osteonal cortical bone; Fracture; Microcrack propagation; Finite element

1. Introduction

Bone mineral density reduction (bone loss), microstructure changes, material properties' variations, and microcrack accumulations all contribute to increased bone fracture susceptibility (Wang et al., 1998; Phelps et al., 2000). Although bone loss has been considered the major cause of bone fractures (Burstein et al., 1976), the contributory effects of microstructure, material properties, and microcrack propagation may require more in-depth investigation (Wang et al., 1998; Guo et al., 1998).

Both in-vivo and in-vitro experiments provided reports on human cortical bone microcracks (Burr and Stafford, 1990; Schaffler et al., 1994). Although various experiments have described the relation between microstructure morphology, bone strength, bone type, aging, and microcrack propagation (Yeni et al., 1997, 1998; Yeni and Fyhrie, 2002), nevertheless, the importance of microcracks has not yet been fully understood.

In osteonal cortical bone, lamellar layers create secondary osteons by surrounding the Haversian canal cylindrically. An incoherent tissue known as interstitial bone fills the space between the osteons. An osteon consists of 10–30 concentric lamellae, each having a thickness of 3–7 μm, surrounding the Haversian canal whose diameter is 30–50 μm. There is a thin amorphous interface between osteon and interstitial bone, known as the cement line, whose material properties are yet to be fully established (Prendergast and Huiskes, 1996).

Secondary osteons in cortical bone could reduce stiffness and strength compared to primary cortical bone. However, osteons could help stop microcrack propagation (Guo et al., 1998; Akkus et al., 1999; O'Brien et al., 2005). The cement line's weak interface, on the other hand, will result in osteon separation from interstitial bone. This tends to deviate or stop microcrack propagation, and thereby increase bone toughness (Saha and Hayes, 1977).

*Corresponding author. Tel.: +1 217 333 0068; fax: +1 217 244 5705.
E-mail address: manssour@uiuc.edu (M.H. Moeinzadeh).

0021-9290/$ - see front matter © 2007 Elsevier Ltd. All rights reserved.
doi:10.1016/j.jbiomech.2007.01.017

The cortical bone is considered a fibre-reinforced composite material (Guo et al., 1998; Hogan, 1992). In such a composite model of the tissue, the osteon is represented by a fibre and interstitial tissue as a matrix. Determination of stress fields around crack tips in such a composite material is conventionally performed using linear elastic fracture mechanics (LEFM). Vashishth et al. (1997), however, showed that resistance to crack growth can arise when toughening mechanisms act within the crack wake (Fig. 1a). This argument led to the current understanding that fracture phenomenon in composite materials such as bone is associated with crack resistance curve (*R*-curve) (Vashishth et al., 1997; Nalla et al., 2005). The subsequent nonlinearity exhibited by the rise in toughness associated with *R*-curve behaviour argues against adoption of LEFM. This was further emphasised by Yang et al. (2006), which states that the existence of microcrack zone at the leading edge of dominant crack, along with the ratio of the microcrack zone length to that of bone thickness, limits the applicability and suitability of LEFM theory.

It might therefore be expected to be able to apply the same argument to a situation where the dominant crack is at the micro-scale. For such an argument to be valid, it is necessary to encounter some form of microcrack zone at the leading edge of dominant microcrack. This would be accompanied by toughening effect and consequently *R*-curve behaviour. There, however, is no tangible evidence that a microcrack zone is formed around the microcrack tip (Fig. 1b). Therefore the *R*-curve phenomenon is not expected to take place at the tip of the microcrack. This could be considered as a sound justification for a return to LEFM and assuming the validity of this theory in microcrack studies.

In this paper, Haversian (osteonal) cortical bone is considered a fibre reinforced composite material governed by the LEFM theory and the finite element method is used for the analysis. The objective is to study the effects of microstructure and bone mechanical characteristics upon fracture phenomenon and the microcrack propagation trajectory.

2. Materials and methods

In the following model, osteons are considered as fibres since they are approximately circular and are parallel to the bone's longitudinal axis (Fig. 2a). The interstitial tissue, which fills the space between the osteons, is considered a matrix (Fig. 2a). The cement line or interface between the osteon and the interstitial tissues is included in the model (Fig. 2a). As suggested by Hogan (1992), the model for a single osteon can be simplified to a quarter circle. This is based on the assumed axisymmetric nature of an osteon. In this model the osteonal fibre area is considered approximately 70% of the total area (Hogan, 1992).

It should, however, be pointed out that the following assumptions are made: 1-plane strain condition, 2-modelling osteonal structures as hollow cylinders and 3-homogenous and isotropic material properties.

Mechanical properties of bone constituents are greatly affected by such factors as bone type and anatomical location. The average elastic moduli in human diaphyseal femoral bone, for example, are found to be 19.3 ± 5.4 GPa in osteonal and 21.2 ± 5.3 GPa in interstitial lamellae (Zysset et al., 1999). In the neck, the average moduli are 15.8 ± 5.3 GPa in osteonal, and 17.5 ± 5.3 GPa in interstitial lamellae (Zysset et al., 1999). Values of 10–19 GPa for osteonal effective elastic modulus (E_o) and 10–26 GPa for interstitial tissue elastic modulus (E_i) are thus adopted to evaluate the effect of mechanical properties upon microcrack behaviour. Here, Poisson's ratio for the osteon and the interstitial bone is assumed to be 0.3 (Hogan, 1992).

The mechanical characteristics of the cement line tissue have also been the subject of different studies. A series of reports such as that produced by Burr et al. (1988), consider this tissue softer than surrounding tissues. Other studies of similar nature, raise the possibility of the tissue viscous characteristics (Lakes and Saha, 1979). Other researchers such as Curry (1984) suggest a more mineralised structure and thus a higher modulus of elasticity. In this paper, following the suggestion made by Advani et al. (1987), the simulation is repeated twice for values of 6 and 24 GPa with the assumed Poisson's ratio of 0.4 (Hogan, 1992).

The computer program Casca Version 1.4 is used to produce a two-dimensional mesh while fracture analysis is performed using Franc 2D. Triangular elements with six nodes or square elements with eight nodes are used to produce the finite element mesh structure.

Simulation of the finite element model is performed for three distinct cases. The first case is the Static Analysis of the model. The geometrical attributes of the model are: (i) osteon radius of 100 μm, (ii) Haversian canal radius of 30 μm, and (iii) thickness of the cement line of 1 μm. Here a crack-free quarter osteon model is presented as shown in Fig. (2b). The model boundary conditions are shown in Fig. (2b). Transverse normal stress in the boundary is taken as 15 MPa (Hogan, 1992). Furthermore, the displacements of the boundary nodes are constrained so that the boundaries remain straight and parallel to their initial states during the deformation period. The intention is to maintain the condition of material continuity. Static analysis is performed on the model using Franc 2D. The objective is to validate the model boundary conditions against that which

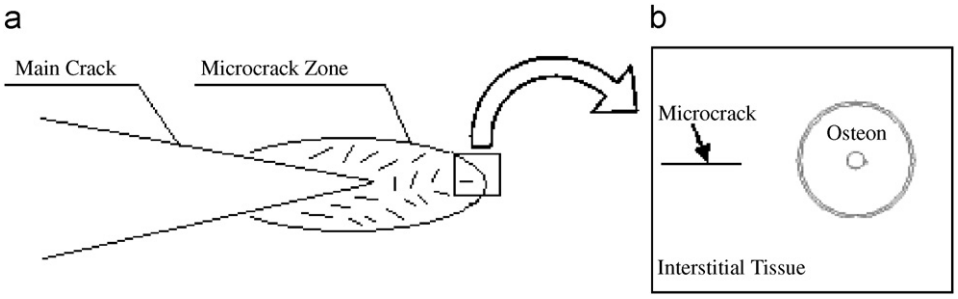

Fig. 1. Schematic diagram representing fracture phenomenon in bone: (a) formation of a microcrack zone at the tip of the main crack and (b) a microcrack close to an osteon.

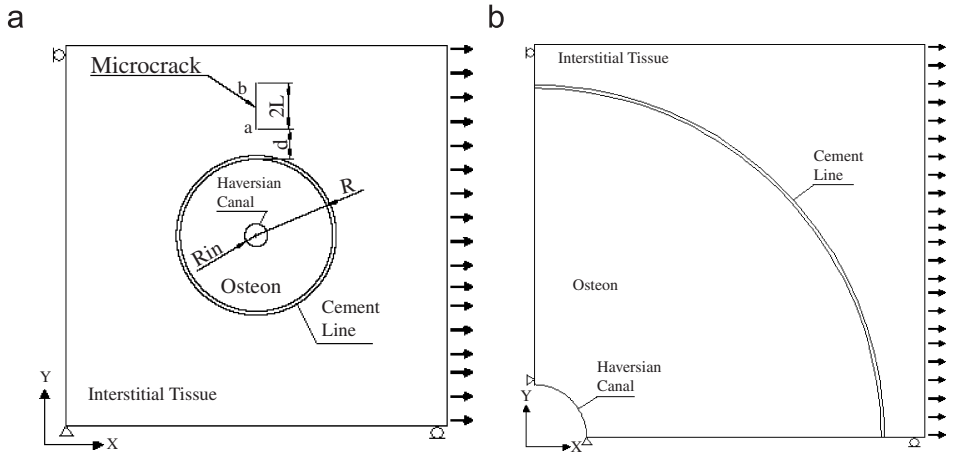

Fig. 2. Fibre reinforced composite micromechanical model for the Haversian cortical bone: (a) model for a single microcrack within the interstitial tissue and (b) quarter model.

is published on microlevel stress distribution (Hogan, 1992; Prendergast and Huiskes, 1996).

In the second case, an internal crack of 30–150 μm in length (Fig. 2a), placed in a vertical orientation to the external loading and directed towards the centre of an isolated single osteon is considered. The boundary conditions are similar to that of the first case. The fracture analysis on the model is also performed by Franc 2D software. The effect of microstructure and mechanical material properties on the stress intensity factor (SIF) is analysed and its magnitude is then measured using the boundary conditions.

The third case is allocated to the analysis of fracture propagation. Here the effect of microstructure upon microcrack propagation trajectory is studied using a model with one, two or multiple osteons. To achieve this, internal and edged microcracks are considered. Similar boundary conditions to that of other cases are assumed. The loading is both tensile and compressive. Franc 2D is used to obtain the microcrack propagation trajectory. Here maximum hoop stress is adopted to determine the propagation direction. Hoop stress (σ_θ) is determined around the crack tip on the circumference of a constant radius circle. The crack propagation is in the direction that is associated with maximum hoop stress. The corresponding mathematical description is provided by expressions (1) and (2).

$$\frac{\partial \sigma_\theta}{\partial \theta} = 0, \tag{1}$$

$$\frac{\partial^2 \sigma_\theta}{\partial \theta^2} < 0. \tag{2}$$

3. Results

3.1. Static analysis

With the loading of $\sigma_{xx} = 15\,\text{MPa}$ (macro-level), the highest stress value (45.75 MPa), is found to be associated with the Haversian canal surface on point B, as shown in Fig. 3. The stress distribution in the vicinity of both the cement line and the Haversian canal boundaries are observed to portray major discontinuities. In addition, large stress changes occur on the Haversian canal boundary.

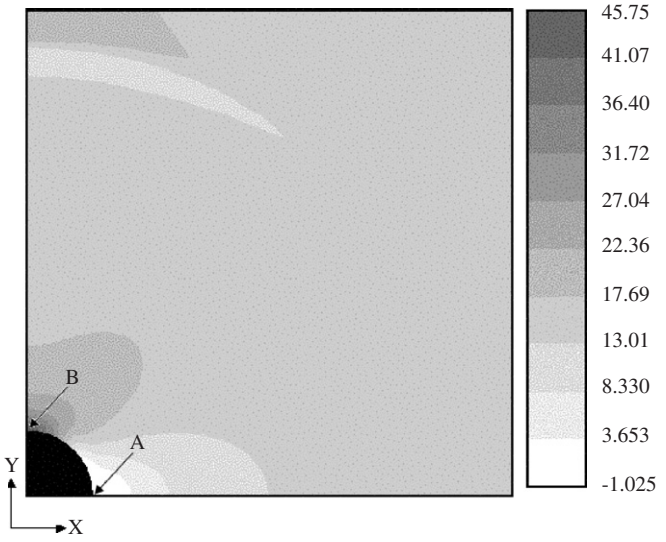

Fig. 3. Variations in microlevel stress (MPa) in the X-direction due to tensile loading of $\sigma_{xx} = 15\,\text{MPa}$. The cement line and the osteon were softer than the interstitial tissue. Smallest and largest microlevel stresses in the X-direction are observed at points A and B, respectively. $E_o = 10\,\text{GPa}$, $E_i = 15\,\text{GPa}$, and $E_c = 6\,\text{GPa}$.

3.2. Fracture analysis

In Fig. (2a), assuming that the osteon is softer than the interstitial tissue (soft osteon, $E_o = 12\,\text{GPa}$, $E_i = 15\,\text{GPa}$), the SIF is increased when d, the crack distance to the osteon boundary, was reduced (Fig. 4). The SIF will, however, decrease if the osteon is stiffer than the interstitial tissue (stiff osteon, $E_o = 12\,\text{GPa}$, $E_i = 10\,\text{GPa}$) (Fig. 4). The next step introduces a cement line into the model. Here, two possible alternative situations have to be considered. In the first case, both the cement line and the interstitial tissue are assumed either stiffer or softer than the osteon. The resulting simulation indicates that the osteon's effect on the SIF is very small and limited to the osteon's vicinity (Fig. 5). In the second case, both cement

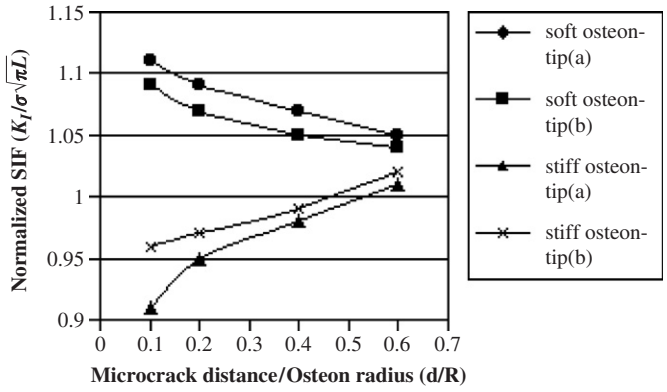

Fig. 4. Normalised SIF variations in constant length crack tips vs. normalised microcrack distance from the osteon, when cement line was not considered. $R = 100\,\mu m$, $\sigma_{xx} = 15\,MPa$, $L = 15\,\mu m$.

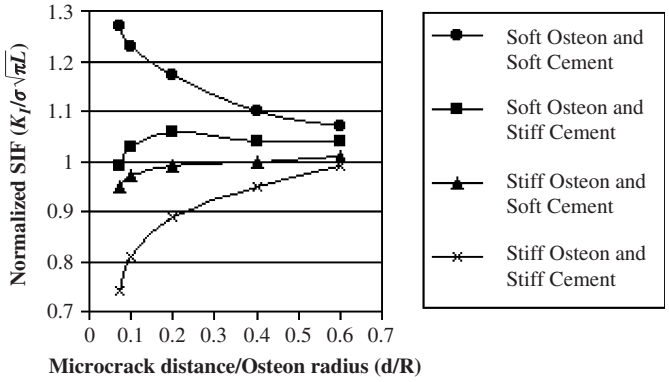

Fig. 5. Normalised SIF in the constant length proximal crack tip (tip a), vs. the normalised microcrack distance from the osteon. The osteonal effect on the microcrack in the vicinity of the osteon is apparent. $R = 100\,\mu m$, $\sigma_{xx} = 15\,MPa$, and $L = 15\,\mu m$.

line and osteon are assumed to be either stiffer or softer than the interstitial tissue. The simulation results, as indicated by Fig. 5, show that the osteon's effect on the microcrack tips SIF is appreciably larger.

3.3. Fracture propagation analysis

In fracture propagation analysis, the edge microcrack is vertical to the loading (Fig. 6a). Within the adopted range of elastic moduli for different tissues, microcrack trajectories deviated from the osteon (Fig. 6b–d). The deviation is, however, reduced as the osteon elastic modulus (E_o) is reduced. When a microcrack is in the same direction as the compressive loading in the interstitial tissue (Fig. 7), the microcrack appears to enter the osteon directly, as shown in Fig. 7. Here, the propagation trajectory is parallel to the applied compressive loading.

In the next step, the model explored two osteons under tensile loading. The crack propagation is found to follow a trajectory between the two osteons. The crack behaves as if it preferred not to enter an osteon (Fig. 8).

The model further explored a number of osteons in the interstitial tissue region. It is found that if an internal microcrack is between any two osteons, the osteons affect the crack propagation. As shown in Fig. 9, it appears that the internal microcrack did not propagate through the space between the osteons, when the distance between the osteons was very small.

4. Discussion

4.1. Static analysis

The static analyses show that the microlevel stresses on the surface of Haversian canal and on the cement line exhibit sudden changes. The Haversian canal is a hole and by the loading described, one would expect that the stress would be approximately three times the far-field stress (45 MPa). This is what the results show in Fig. 3. These results are in accordance with what was reported by Hogan (1992). It should be noted that other porosities, such as that of Volkmann's canal which could affect microlevel stresses, are not included. It should also be pointed out that the cement line characteristics are far more complex than that of an elastic material. This complexity could manifest itself in the shape of viscoelastic behaviour. Such characteristics could affect the stress variation on the cement line. These variations in the stress could also stem from perfect bonding assumption. In general, to predict exact microlevel stress variations, a rather more detailed set of data regarding the cortical bone material constituents is required.

4.2. Fracture analysis

In this paper the Haversian cortical bone micromechanics and the effects of the material properties, morphology and microstructure upon fracture phenomenon have been studied. The microcracks are assumed to be inside the interstitial tissue since the majority of microcracks are found within this tissue in in-vivo observations (O'Brien et al., 2005). Furthermore, the current studies include fracture phenomenon and microcrack growth before encountering the cement line. That is why the concept of cement line debonding is excluded in the current paper.

Formation of frontal process zone and the consequential process zone wake in the vicinity of the microcrack tip have not as yet been substantiated. This points away from *R*-curve phenomenon, and thus permits adoption of LEFM.

At the microcrack tip, existence of diffused damage in the form of delamination at the lamellar level and mineralised collagen fibril failure at the ultrastructural level, is established (Diab and Vashishth, 2005; Vashishth et al., 2000) but whether or not the diffused damages result in *R*-curve phenomenon is not clear. The possible effects of diffused damages on the adoption of LEFM are therefore not addressed in this paper.

The results indicate that microstructural heterogeneity has a direct bearing upon the fracture behaviour of the Haversian cortical bone. The reason being, that osteons'

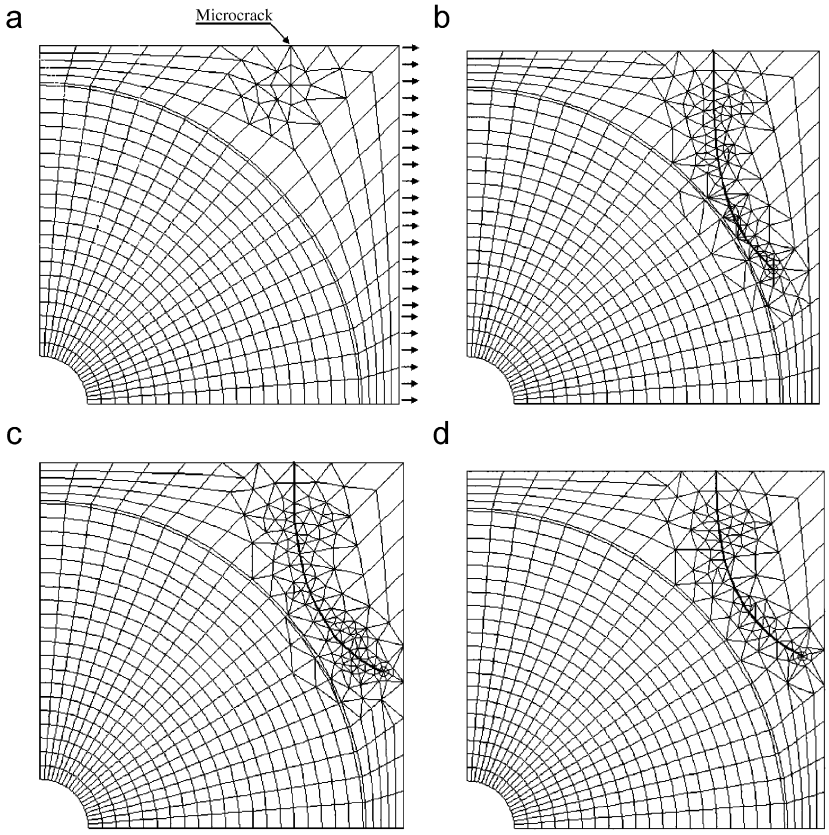

Fig. 6. Microcrack propagation trajectory under tension—the propagation microcrack trajectory was deviated as it approached the osteon. (a) Primary microcrack, and (b, c, d) propagation microcrack; (b) $E_o = 10\,GPa$, $E_i = 26\,GPa$, $E_c = 6\,GPa$; (c) $E_o = 19\,GPa$, $E_i = 26\,GPa$, $E_c = 6\,GPa$; (d) $E_o = 19\,GPa$, $E_i = 15\,GPa$, $E_c = 24\,GPa$.

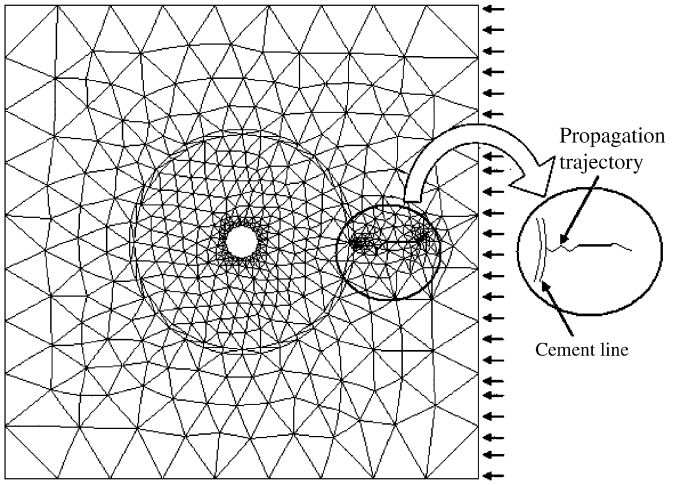

Fig. 7. Microcrack propagation trajectory under compression. The microcrack enters the osteon directly in a direction parallel to that of loading.

effect on microcracks changes with changes in mechanical properties of different tissues in microstructure. This supports the points raised in previous articles (Phelps et al., 2000; Guo et al., 1998). The results also indicate that, if the cement line and the osteon are assumed to be softer than the interstitial tissue, the SIF is increased when the crack distance to the osteon boundary is reduced. The SIF will, however, decrease if the osteon and cement line are stiffer than the interstitial tissue. Changes in tissue mechanical material properties could also change the SIF. This will affect the fracture phenomenon. The aging process, for example, makes the interstitial tissue stiffer (Crofts et al., 1994). This could be considered as yet another factor affecting the fracture behaviour of the tissue (Phelps et al., 2000; Guo et al., 1998). It may therefore, be possible to conclude that such changes in the mechanical properties of different tissues make the bone more prone to fracture.

4.3. Fracture propagation analysis

The microcrack growth trajectory is also influenced by both the microstructure of the Haversian cortical bone and loading conditions. An osteon could repel microcracks during tensile loading. Deviation takes place regardless of whether osteons are softer or harder than interstitial tissue. This phenomenon occurs within the range of elastic moduli which are adopted for individual tissues. The deviation is, however, reduced as osteon elastic modulus (E_o) is reduced. This is found to be in contrast to what was reported by Guo et al. (1998), who suggested that only hard osteons repel microcracks. Incremental reduction of osteonal

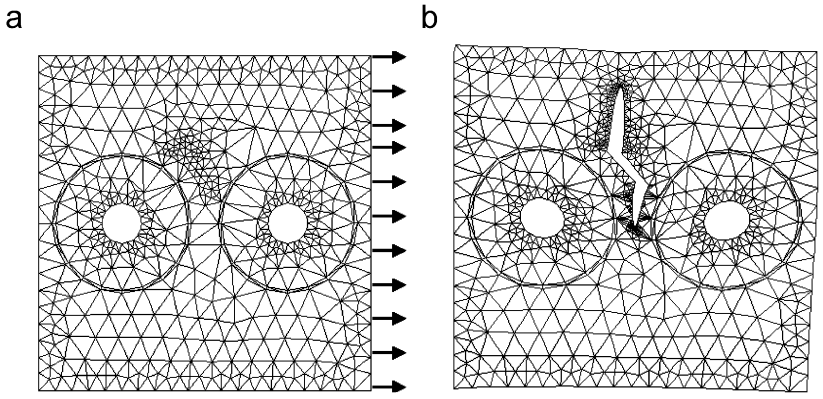

Fig. 8. Microcrack propagation in between osteons during tensile loading: (a) primary microcrack and (b) propagation microcrack.

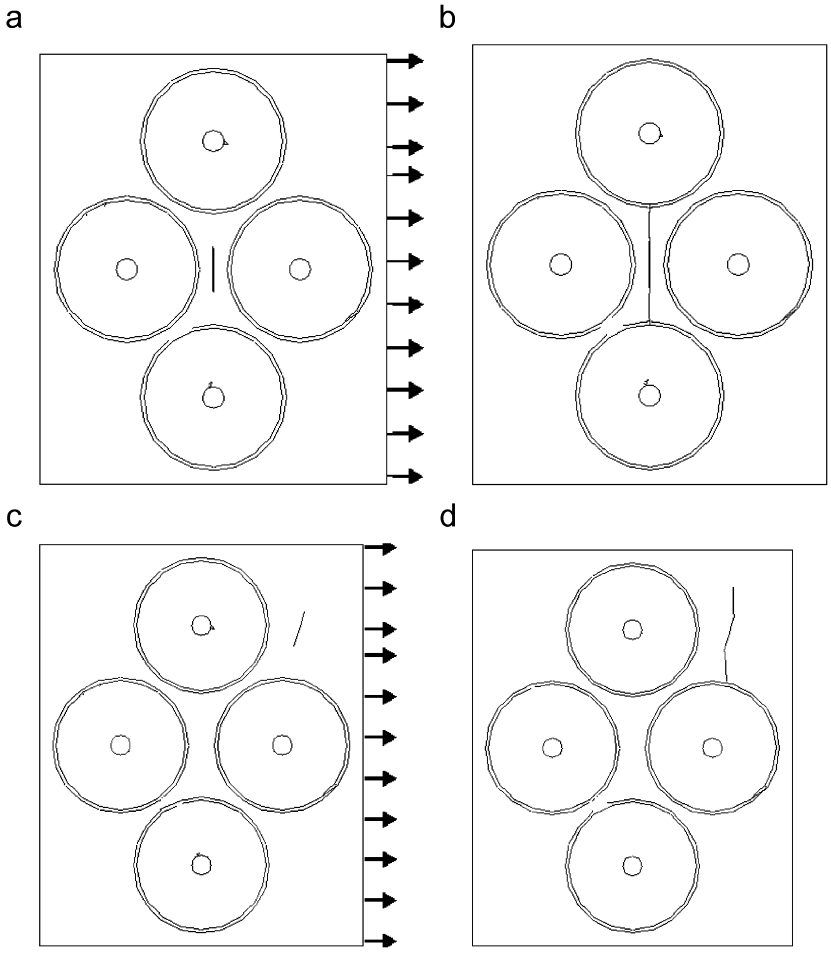

Fig. 9. Microcrack propagation (under tensile loading) was severely affected by the separation of the osteons. Close proximity of osteons will not allow microcrack propagation to take place in between the osteon. (a) and (c) primary microcrack and (b) and (d) propagation microcrack.

elastic modulus (E_o) in the current model, also leads the osteon attracting the microcrack. This behaviour, however, can only be observed when theoretical values used for E_o are well outside the range of experimental results.

Furthermore, the results of this study indicate that osteons behave as a barrier to microcrack growth (Figs. 6 and 8). Short cracks are therefore encountered more frequently than long cracks in this tissue (Schaffler et al., 1994). Other researchers have also reported similar observations in experimental studies. Experiments performed by O'Brien et al. (2005), also suggest that microcracks smaller than 300 μm are deviated in the

vicinity of the osteon or they are stopped at the cement line. Fracture surface studies, on the other hand, indicate that if microcracks can grow up to a particular length (approximately 300 μm), in Haversian cortical bone, they can then penetrate osteons (O'Brien et al., 2005). If these cracks continue to grow through the concentric lamellae inside an osteon and have a high enough stress intensity value to break through Haversian canal, they have a clear pathway with no barriers to further growth and failure is the likely results (O'Brien et al., 2005). This could quite possibly explain the findings of fracture surface studies where failure surfaces tend to show splitting of osteons, often at the centre of Haversian canals. Therefore, both microcrack deviation as it approaches the osteon and its halt on the cement line boundary cause growth reduction and refrain its penetration into the osteon. Both these phenomena enhance Haversian cortical bone resistance to fracture.

If, however, the microcrack and the compressive loading are in the same direction, the microcrack is expected to enter the osteon. The SEM results of experimental fracture surface studies also indicate that microcracks enter the osteon in the same direction as the compressive loading (Burr and Stafford, 1990; Reily and Currey, 2000). The microcracks caused by compressive loadings are consequently long and straight (Boyce et al., 1998; Burr et al., 1998).

As previously noted, the microcrack growth is affected by the osteons and it follows a path between them. This path is also affected by the distance between the osteons. Multi-osteonal models show that microcrack growth slowed and eventually approached a complete halt when distances between osteons were small. Other experimental results suggest that microcracks stop once they enter a high osteon density bone tissue (O'Brien et al., 2005), a point directly related to bone toughness. The current model however, does not provide for osteon pullout and cement line debonding. These phenomena affect the bone toughness (Guo et al., 1998; O'Brien et al., 2005; Saha and Hayes, 1977).

In conclusion, material properties and morphological parameters of the microstructure greatly influence the bone's fracture behaviour. This paper emphasises the effect of tissue properties differences upon fracture phenomena. Osteon effect on microcrack trajectories and increased bone toughness are considered as other points of particular interest. However, to improve the current model and enhance the understanding of the fracture in the Haversian cortical bone, it is necessary to include the concepts of cement line debonding and osteonal pullout.

References

Advani, S.H., Lee, T.S., Martin, R.B., 1987. Analysis of crack arrest by cement lines in osteonal bone. In: Erdman, A.G. (Ed.), 1987 Advances in Bioengineering, vol. 3. ASME, New York, BED, pp. 57–88.

Akkus, O., Davy, D.T., Rimnac, C.M., 1999. Microdamage coalescence mechanisms in human cortical bone. In: 23rd Annual meeting of the American Society of Biomechanics, University of Pittsburgh, October, 21–23.

Boyce, T.M., Fyhrie, D.P., Glotkowski, M.C., Radin, E.L., Schaffler, M.B., 1998. Damage type and strain mode association in human compact bone bending fatigue. Journal of Orthopaedic Research 16, 322–329.

Burr, D.B., Stafford, T., 1990. Validity of the bulk-staining technique to separate art factual from in vivo microdamage. Clinical Orthopaedics and Related Research 260, 305–308.

Burr, D.B., Schaffler, M.B., Fredericson, R.G., 1988. Composition of the cement line and its possible mechanical role as a local interface in human compact bone. Journal of Biomechanics 21, 939–945.

Burr, D.B., Turner, C.H., Naick, P., Forwood, M.R., Ambrosius, W., Sayeed Hasan, M., Pidaparti, R., 1998. Does microdamage accumulation affect the mechanical properties of bone? Journal of Biomechanics 31, 337–345.

Burstein, A.H., Reilly, D.T., Martens, M., 1976. Aging of bone QJ;tissue: mechanical properties. Journal of Bone Joint Surgery 58-A, 82–86.

Crofts, R.D., Byoce, T.M., Milgrom, C., 1994. Aging changes in osteon mineralization in the human femoral neck. Bone 15, 137–152.

Curry, J., 1984. The Mechanical Adaptations of Bones. Princeton University Press, New York.

Diab, T., Vashishth, D., 2005. Effects of damage morphology on cortical bone fragility. Bone 37, 96–102.

Guo, X.R., Liang, L.C., Goldstein, S.A., 1998. Micromechanics of osteonal cortical bone fracture. Journal of Biomechanical Engineering 120, 112–117.

Hogan, H.A., 1992. Micromechanics modelling of Haversian cortical bone properties. Journal of Biomechanics 25 (5), 549–556.

Lakes, R., Saha, S., 1979. Cement line motion in bone. Science 204, 501–503.

Nalla, R.K., Kruzic, J.J., Kinney, J.H., Ritchie, R.O., 2005. Mechanistic aspects of fracture and *R*-curve behavior in human cortical bone. Biomaterials 26 (2), 217–231.

O'Brien, F.J., Taylor, D., Lee, T.C., 2005. The effect of bone microstructure on the initiation and growth of microcracks. Journal of Orthopaedic Research 23, 475–480.

Phelps, J.B., Hubbard, G.B., Wang, X., Agrawal, C.M., 2000. Microstructural heterogeneity and the fracture toughness of bone. Journal of Biomedical Material Research 51, 735–741.

Prendergast, P.J., Huiskes, R., 1996. Microdamage and osteocyte-lacuna strain in bone: a microstructural finite element analysis. Journal of Biomechanical Engineering 118, 240–246.

Reily, G.C., Currey, J.D., 2000. The effects of damage and microcracking on the impact strength of bone. Journal of Biomechanics 33, 337–343.

Saha, S., Hayes, W.C., 1977. Relation between tensile impact properties and microstructure of compact bone. Calcified Tissue Research 24, 65–72.

Schaffler, M.B., Pitchford, W.C., Choi, K., Riddle, J.M., 1994. Examination of compact bone microdamage using back-scattered electron microscopy. Bone 15 (5), 483–488.

Vashishth, D., Behiri, J.C., Bonfield, W., 1997. Crack growth resistance in cortical bone: concept of microcrack toughening. Journal of Biomechanics 30 (8), 763–769.

Vashishth, D., Tanner, K.E., Bonfield, W., 2000. Contribution, development and morphology of microcracking in cortical bone during crack propagation. Journal of Biomechanics 33, 1169–1174.

Wang, X.D., Masilamani, N.S., Mabry, J.D., Alder, M.E., Agrawal, C.M., 1998. Changes in the fracture toughness of bone may not be reflected in its mineral density, porosity and tensile properties. Bone 23 (1), 67–72.

Yang, Q.D., Cox, B.N., Nalla, R.K., Ritchie, R.O., 2006. Fracture length scales in human cortical bone: the necessity of nonlinear fracture models. Biomaterials 27, 2095–2113.

Yeni, Y.N., Fyhrie, D.P., 2002. Fatigue damage-fracture mechanics interaction in cortical bone. Bone 30 (3), 509–514.

Yeni, Y.N., Brown, C.U., Wang, Z., Norman, T.L., 1997. The influence of bone morphology on fracture toughness of the human femur and tibia. Bone 21 (5), 453–459.

Yeni, Y.N., Brown, C.U., Norman, T.L., 1998. Influence of bone composition and apparent density on fracture toughness of the human femur and tibia. Bone 22 (1), 79–84.

Zysset, P.K., Guo, X.E., Hoffler, C.E., Moore, K.E., Goldstein, S.A., 1999. Elastic modulus and hardness of cortical and trabecular bone lamellae measured by nanoindentation in the human femur. Journal of Biomechanics 32, 1005–1012.